Electronic structure of YbN

L. Degiorgi, W. Bacsa, and P. Wachter

Laboratorium für Festkörperphysik, Eidgenössische Technische Hochschule Zürich, 8093 Zürich, Switzerland

Large single crystals of cubic and stoichiometric YbN have been grown. On these crystals we measured the optical reflectivity for photon energies between 1 meV and 12 eV, also at helium temperatures, and performed a Kramers-Kronig analysis to obtain the optical constants. In addition, we measured the Raman effect to obtain further information on the phonon spectra. The electrical conductivity at room and at low temperature and the Hall effect at 300 K served to obtain also the effective mass of the carriers. Also the magnetization and initial susceptibility have been measured. The main important results are that YbN is a self-compensated semimetal with about 10^{20} carriers per cm^{-3}, the occupied $4f^{13}$ state is about 6 eV below E_F, the empty $4f^{14}$ state is about 0.2 eV above E_F, and the effective mass of the carriers is about $2.2m_e$. In other words the material definitely is not a heavy fermion—but more probably a Kondo system. Nonstoichiometric samples tend to show stronger Kondo features.

INTRODUCTION

The electronic structure of the rare-earth pnictides is a continuous matter of debate. On the theoretical side the coexistence of localized $4f$- and extended band states makes a simultaneous description in a band-structure calculation very difficult, if not impossible.[1] To avoid these problems, band-structure calculations are often performed for the pnictides with only the end members of the lanthanide series which have empty or completely occupied $4f$ shells.[2,3]

The experimental situation is also rather complex, mainly because of generally imperfect materials. In the early sixties the pnictides were polycrystalline, partially oxidized, and nonstoichiometric. They were generally considered metals with magnetization, neutron scattering, and specific heat as useful measurements.[4,5] Sclar[6] was the first to prepare rare-earth pnictides in the form of thin films also performing optical and electrical measurements on them. He claimed that rare-earth nitrides were semiconductors and thus started a 20-year-long debate. Having misinterpreted the direct p-d transition at the Γ point as the absorption edge of a semiconductor, Sclar's results were compromised.

The next step was the preparation of stoichiometric polycrystalline rare-earth nitrides and substantiating the preparation by chemical analysis ($\pm 0.5\%$). However, even then, several puzzles remained. GdN, being isostructural and isomagnetic with the ferromagnetic semiconductor EuO, never was found to be semiconducting as was considered possible for a III-V compound.[4] This question has only been solved after the preparation of large (several mm edge length), stoichiometric single crystals, where the carrier concentration could be determined unambiguously with the Hall effect and optical reflection.[7,8] In this situation it has been shown for the first time that GdN is a metamagnet with a T_N of 40 K, i.e., that it is no longer isomagnetic with EuO, and that the carrier concentration at 300 K is 6% per Gd ion, far

above any possible error in the chemical analysis of the stoichiometry. In the meantime, carrier concentrations of a few percent per cation have been found for many of the rare-earth pnictides.[9]

Within the nitrides the compounds without occupied $4f$ states, i.e., ScN, YN, LaN, and the complete $4f$ shell as in LuN have the highest chance of becoming semiconducting with a gap between the p valence band originating in nitrogen orbitals and the $d(s)$ conduction band of the rare-earth metal; namely, the $4f$ states as with the rare-earth metals, will be between 2 and 10 eV below E_F,[10] and thus in general will hybridize with the p bands (p-f mixing). As seen by second-order perturbation theory, the p-f interaction will then shift the p bands upwards (in addition to creating a hybridization gap within the p bands) thus diminishing a possible p-$d(s)$ gap and provoking instead a p-d overlap.

We have thus investigated already ScN (Ref. 11) with such perfect stoichiometry and stability that the single crystals could be boiled for hours in a mixture of HNO_3 and H_2SO_4 before being dissolved. The compound exhibited metallic behavior, having a carrier concentration of about 10^{20} cm^{-3} at room temperature.

All the rare-earth pnictides crystallize in the fcc rocksalt structure, and thus symmetry considerations tell us that the anion p^6 valence bands have their maximum at the Γ point of the Brillouin zone. In this close-packed crystal structure the ligand field on the cation $5d$ orbitals is so large that the bottom of the conduction band will be formed by the $5dt_{2g}$ derived state, and not by the $6s$ derived states. The $5d$ band has its minimum at the X point of the Brillouin zone. Thus when the pnictides behave as metals, as experimentally verified, there exists an indirect overlap of the p and d band and the materials are semimetals. Under this condition the concentration of holes in the p band equals those of the electrons in the d band resulting in self-compensation. On the other hand the band overlap is so small that the carrier concentration will be only a few percent and thus may be in the order of

a possible off-stoichiometry.

This is the reason why the perfection and quality of the rare-earth pnictides is so important. A change in stoichiometry of only 1% may change the carrier concentration by 100% and thus influence all physical parameters like lattice constant, magnetic, and optical properties, and electrical conductivity. As has been discussed previously in the case of GdN increased stoichiometry changed the magnetic behavior from ferromagnetism to metamagnetism with the ordering temperature decreasing from 70 K towards 40 K.[7] The next interesting case (besides intermediate valent CeN) is YbN (or more generally the Yb pnictides) which have been suggested to be heavy fermions.[12] On the other hand, recent photoemission measurements on YbN and their analysis lead to the conclusion that YbN is integer valent with a pure $4f^{13}$ configuration.[13]

It is the aim of the present paper to shed some light on the valence configuration and the electronic structure of YbN by performing several physical measurements on the same, chemically well-characterized single crystal of YbN. As a result it can be clearly stated that YbN is slightly intermediate valent and it is not a heavy fermion.

SAMPLE PREPARATION

The detailed experimental procedure has been described in earlier publications.[14] The main points are that the handling of the metal and the compound has been performed in argon glove boxes gettered by hot cerium turnings having a residual oxygen concentration of less than 3 ppm. Commercially available 99.99% sublimed Yb metal has been transformed into metal turnings and prereacted in an open and cleaned Mo crucible for 12 h at 1900° C in a nitrogen stream. The resulting polycrystalline material has been reground in the glove box and nitrided again for 12 h and the same procedure repeated again. The compound had a lattice constant of 4.781 Å and even after 24 h of x-ray irradiation only the rocksalt structure could be detected. The material has been analyzed with a micro Kjeldahl method[15] for its nitrogen content and was found to be stoichiometric (±0.5%). This prereacted material has been put into a tungsten crucible with a temperature gradient of 1940°C and 1970°C between top and bottom and has been kept at this temperature for 11 days and then slowly cooled. Large single crystals between 3-mm and 5-mm edge length had grown. Within the precision of the chemical analysis no nitrogen had been lost. Several single crystals from this crucible have been cleaved in the glove box and been transferred without contamination with air to optical spectrometers where their reflectivity has been measured. The spectral position of the plasma edge minimum determines the carrier concentration and thus the crystal with the lowest energy of the plasma edge has been selected for further measurements. This procedure assumes that any off-stoichiometry or impurity creates additional carriers and thus the material with the lowest carrier concentration is the best. This method is more precise than the chemical analysis. For comparison we made also some measurements on a nonstoichiometric

single crystal which had a lattice constant of 4.784 Å and a composition of $YbN_{0.96}$.

EXPERIMENTAL RESULTS

The optical reflectivity of YbN has been measured in a photon energy range from 12 eV down to 1 meV at room temperature (and in the infrared spectral range also at 6 K) using three spectrometers. Generally we use in the uv region in situ cleaved crystals, but since we concentrate in this investigation on the one crystal with the lowest carrier concentration, we did not want to risk a destruction of the crystal upon cleaving and thus used dry polishing in a vacuum. In the far infrared part of the spectrum we have employed a Fourier spectrometer with triglycene detectors down to 50 cm^{-1} and a liquid-helium cooled germanium bolometer from 100 to 10 cm^{-1}. The whole spectrum at 300 K is shown in Fig. 1(a) with practically no change at 6 K. In addition we show in Fig. 1(a) the infrared part of the reflectivity at 6 K of the non-stoichiometric crystal (the reflectivity at 300 K is practically the same as the stoichiometric crystal). In Fig. 1(b) the visible and uv part of the reflectivity is shown in an expanded scale. In Fig. 1(b) we also show the reflectivity
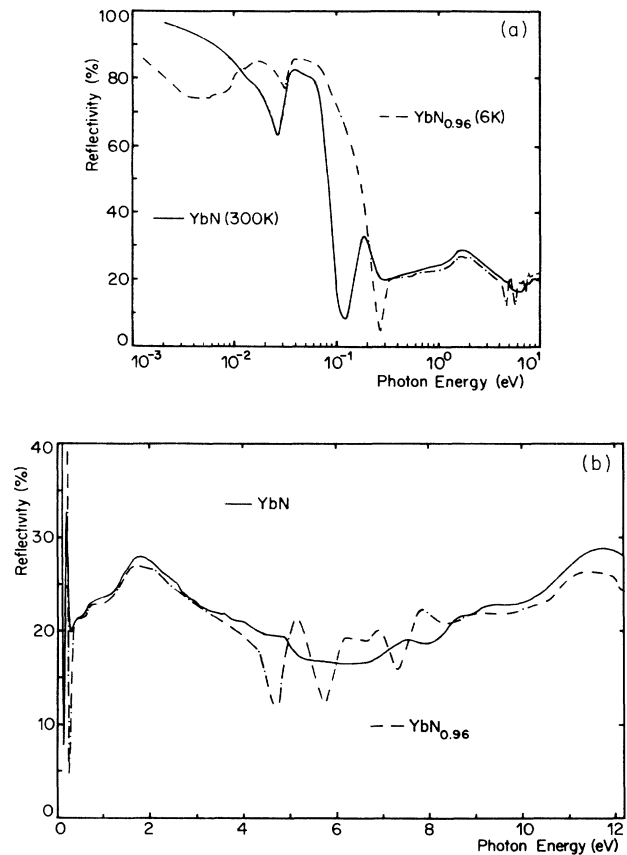

FIG. 1 (a) Optical reflectivity between 1 meV and 12 eV of a stoichiometric single crystal (YbN) at 300 K and a non-stoichiometric single crystal ($YbN_{0.96}$) at 6 K. (b) Optical reflectivity in the high-energy spectral region of stoichiometric YbN and nonstoichiometric $YbN_{0.96}$ at 300 K.

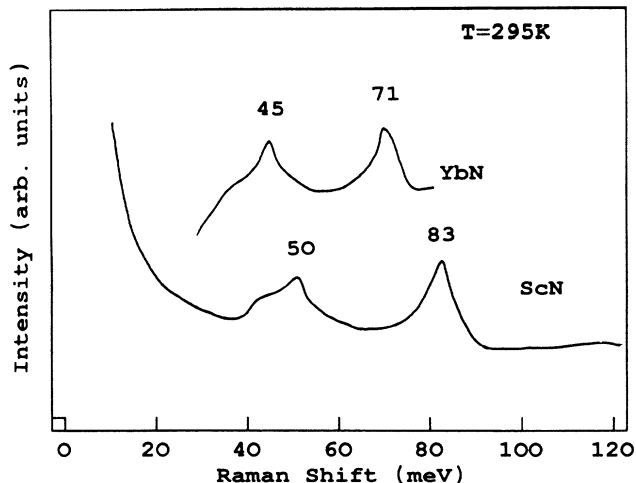FIG. 2. Raman shift of YbN compared with ScN at 300 K.

To enhance the information on phonon properties of YbN we measured also Raman spectra at 300 and 6 K using a 5145-Å laser excitation. In Fig. 2 we compare the result at 300 K with the corresponding measurement on ScN[11] and except a spectral shift find similar results. The rocksalt crystal structure prohibits the first order Raman effect due to symmetry relations. However, always present defects relax the q-selection rule and the Raman effect (when detectable) measures a weighted one-phonon density of states.

To obtain also information on the crystal-field splitting and the magnetic ground state we also measured the magnetic susceptibility in an applied field of 10 kOe and the initial susceptibility in a field of 10 Oe. The result of the inverse magnetic susceptibility is shown in Fig. 3.

the visible and uv part of the nonstoichiometric YbN single crystal which has been cleaved in a vacuum in the spectrometers. In comparison with cleaved ScN (Ref. 11) and cleaved nonstoichiometric YbN it is to be mentioned that the uv part of the spectrum of stoichiometric YbN is less pronounced due to surface destruction with polishing and consequent light scattering.

We also have measured the electrical resistivity of the same stoichiometric crystal with a conventional four-probe method and the Hall effect employing the van der Pauw technique. At room temperature σ_{dc} has been found to be 1.126×10^{16} sec^{-1} with a metallic temperature coefficient, and the negative Hall effect implied a carrier concentration of $N_e = 4.8 \times 10^{20}$ cm^{-3} using an effective one-band model for the interpretation (see discussion). YbN has thus even lower values of the conductivity ($\sigma_{dc} = 2.2 \times 10^{16}$ sec^{-1}) and carrier concentration ($N_e = 5.9 \times 10^{20}$ cm^{-3}) than ScN.[11] Electrical resistivity measurements on the nonstoichiometric YbN probe yielded $\sigma_{dc} = 9 \times 10^{15}$ sec^{-1} at room temperature.
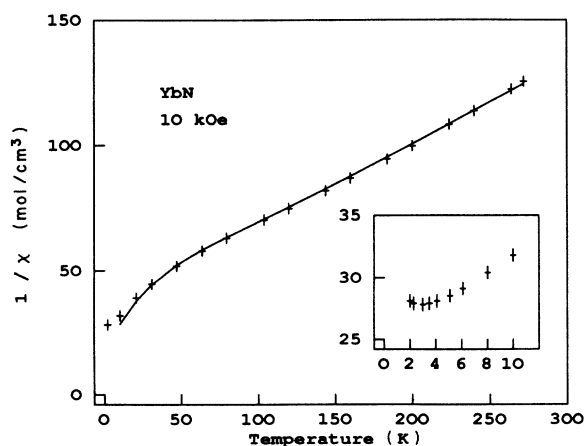
DISCUSSION

Plasmons and Phonons

It has already been mentioned in the introduction that by symmetry considerations the rare-earth pnictides are self-compensated semimetals with an indirect overlap of p and d bands. Band-structure calculations have been reliably performed only for non-rare-earth compounds like ScN and ScP (Refs. 16 and 17), where in Ref. 17 especially also electron-hole correlations have been included. This band structure has been confirmed experimentally on stoichiometric ScN single crystals.[11]

Another major result of such band-structure calculations is a transfer of cation and anion wavefunctions or covalency (charge within or outside a muffin-tin sphere[16]). Whereas the nitrides have the lowest degree of covalency within the pnictides, their covalency is much larger than for the chalcogenides. Point charges of 2 or 3 for these compounds thus bear little relevance, although it is evident that nitrides have a larger point charge than other pnictides.[18] Effective charges can be precisely measured, e.g., in CeO_2 and they agree with the muffin-tin charges.[19,20] Such effective charges have their prime importance in calculating crystal-field splittings and extrapolations from one measured material (e.g., YbAs) to another (e.g., YbN).

The single crystals of our stoichiometric YbN had with 4.781 Å the lowest lattice constant ever measured, starting with 4.792 Å (Ref. 4) and ending with 4.7839 Å.[12] (In passing we want to mention that a stoichiometric material with e.g., $Yb_{0.97}N_{0.97}$ could also have a smaller lattice constant, although we consider this possibility as far fetched.) At the same time the single crystals grown from our prereacted material have the lowest carrier concentration ever measured on YbN.[8] The typical off-stoichiometry in rare-earth nitrides is a nitrogen deficiency.[4,8,12] The lattice collapse around such a nitrogen deficiency for other typical rare-earth nitrides can be estimated to be only 0.005 Å for 5% vacancies.[21] The fact that stoichiometric YbN has a smaller lattice constant than material with nitrogen defects points to another mechanism. Nitrogen deficiency results in the formation of Yb^{2+} and in excess electrons, the former having a larger (1.13 Å) ionic radius than Yb^{3+} (0.94 Å). It is ob-

FIG. 3. Inverse magnetic susceptibility of YbN in a field of 10 kOe. The insert shows details below about 10 K.

ELECTRONIC STRUCTURE OF YbN

vious that the simultaneous presence of Yb^{2+} and Yb^{3+} due to off-stoichiometry will have serious consequences when discussing the possibility of intermediate valence or heavy fermions.[12] For reasons of comparison we have selected also a nonstoichiometric single crystal having a lattice constant of 4.784 Å and a composition of $YbN_{0.96}$ for reflectivity measurements (Figs. 1(a) and 1(b).

A Kramers-Kronig transformation of the optical reflectivity spectrum of Figs. 1(a) and 1(b) has been performed in order to obtain the optical constants ($\hat{\epsilon}=\epsilon_1-i\epsilon_2$, $\hat{\sigma}=\sigma_1-i\sigma_2$). The frequency range of the measured reflectivity spectrum has been extrapolated towards zero frequency by means of the Hagens-Rubens relation

$$R(\omega)=1-(2\omega/\pi\sigma_{dc})^{1/2},\qquad(1)$$

using the measured value of the static electrical conductivity $\sigma_{dc}=1.126\times10^{16}$ sec^{-1} (for the nonstoichiometric sample $\sigma_{dc}=9.10^{15}$ sec^{-1}). For energies larger than 12 eV and up to 18 eV the reflectivity has been assumed to drop off as ω^2, and for still higher energies as ω^4. The dielectric functions obtained are plotted for the measured range in Fig. 4(a) (for stoichiometric YbN at 300 K, for

nonstoichiometric at 6 K) and for stoichiometric YbN the high-energy range is displayed in Fig. 4(b). In Fig. 4(b) we also show the dielectric functions of the cleaved, nonstoichiometric YbN for the high-energy range. The real part (absorptive) of the optical conductivity for stoichiometric YbN is shown for the high-energy region in Fig. 5. The dielectric functions ϵ_1 and ϵ_2 exhibit an interesting anomaly in the infrared region at about 34 meV [Fig. 4(a)], which is shifted towards higher energy for the nonstoichiometric sample, which in addition at low temperatures has another feature at even lower energies.

The analysis of the spectra is complicated by the fact, that besides the intraband absorption due to free carriers (Drude), TO phonons and high-energy interband transitions (resulting in ϵ_{opt}) there are also low-energy d-f interband transitions (to be discussed below) and low-energy transitions of the holes between the three (light mass, heavy mass, spin-orbit mass) different valence bands. All these effects (except d-f transitions) have been taken into account in ScN,[11] because a reliable band-structure calculation was available.[17] No such band-structure calculation exists for YbN. We thus have to resort to a simpler procedure, however, using the knowledge obtained with ScN.[11]

By looking at the reflectivity curve of stoichiometric YbN in Fig. 1(a) we realize that interband tranistions are exhausted near 0.1 eV at which energy we observe a minimum reflectivity due to the plasma edge of the free carriers (0.3 eV for the nonstoichiometric crystal). At about 34 meV this plasma edge is superimposed by a structure due to phonons. By making a comparison with the plasma minimum in ScN,[11] which is near 0.5 eV we realize that the plasma resonance

$$\omega_p'=(4\pi e^2N_e/m_0\epsilon_{opt})^{1/2}\qquad(2)$$

is at much lower energy in stoichiometric YbN. Here N_e is the concentration of electrons being equal to the one of the holes in a compensated system. m_0 is the optical mass of an electron-hole pair.[17] Now ω_p' is the coupled or screened plasma resonance, defined where ϵ_1 has its zero crossing. However, $\hat{\epsilon}$ in the infrared spectral range is
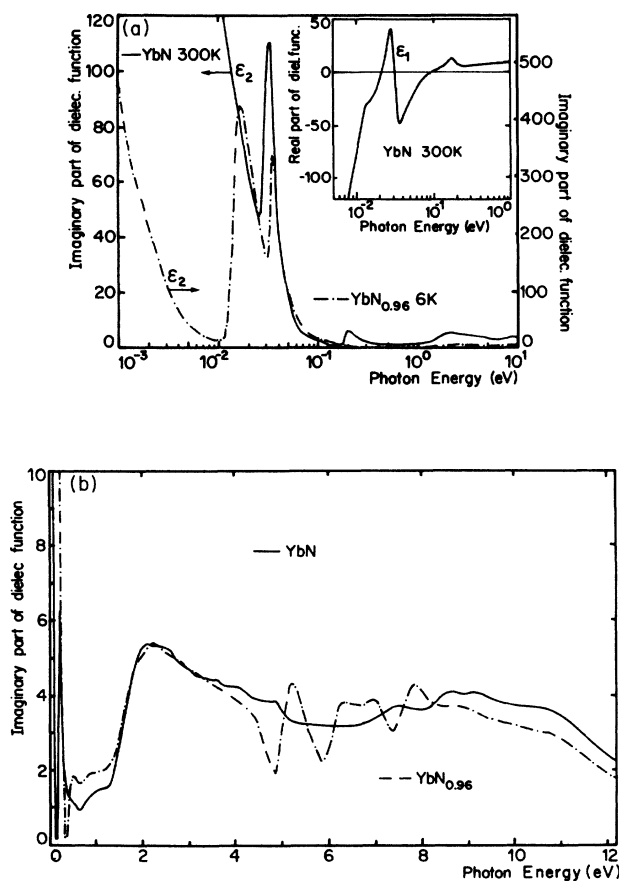

FIG. 4. (a) Imaginary (absorptive) part of the dielectric function of YbN at 300 K and $YbN_{0.96}$ at 6 K. The insert shows the real (dispersive) part of YbN at 300 K. (b) Imaginary (absorptive) part of the dielectric function of YbN and $YbN_{0.96}$ (cleaved) at 300 K for the high-energy spectral region.
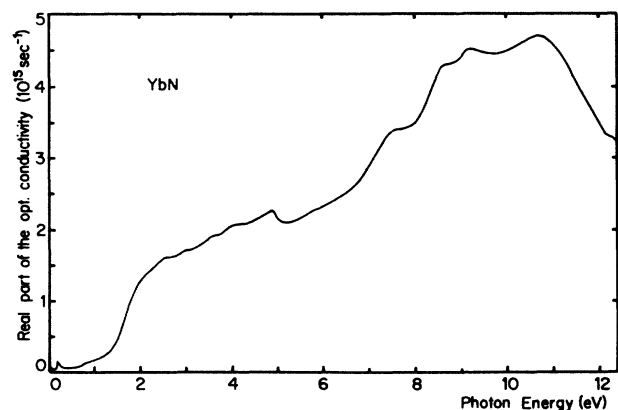

FIG. 5. Real (absorptive) part of the optical conductivity of YbN at 300 K.

composed of at least three contributions—those of the higher-energy interband tranistions manifest in ϵ_{opt}, the free-carrier contribution $\hat{\epsilon}^f$, and that of the phonons. Thus,

$$\hat{\epsilon} = \epsilon_{opt} + \omega_p^2/(-\omega^2 + i\gamma\omega) + \Omega^2/(\omega_{TO}^2 - \omega^2 + i\Gamma\omega) . \quad (3)$$

Here ω_p is the unscreened or decoupled plasma resonance, defined where ϵ_1^f has its zero crossing, ω_{TO} is the transverse-optical phonon frequency, Ω is their oscillator strength and γ, respectively Γ, are damping constants. By means of the Kramers-Kronig relation we can decompose $\hat{\epsilon}$, and the imaginary part of the dielectric constant ϵ_2 is shown in Fig. 6.

The zero crossing of ϵ_1^f and thus the energy of the uncoupled plasma resonance ω_p is at 0.19–0.20 eV in stoichiometric YbN (0.5 eV for nonstoichiometric YbN) and for comparison at 0.8–0.99 eV in ScN.[11] Now

$$\omega_p = (4\pi e^2 N_e/m_0)^{1/2} \quad (4)$$

and is thus proportional to $(N_e/m_0)^{1/2}$. m_0 for ScN has been determined from a band-structure calculation and has been found to be compatible with the experimental results;[11,17] its value is $m_0 \cong 0.13m_e$. Since no such band-structure calculation is available for YbN we can nevertheless derive the optical mass of stoichiometric YbN by comparing it with ScN, using the measured carrier concentration N_e by means of the Hall effect:

$$\frac{(\omega_p^2)^{ScN}}{(\omega_p^2)^{YbN}} = \frac{N_e^{ScN} m_o^{YbN}}{N_e^{YbN} m_o^{ScN}} \cong 21 . \quad (5)$$

We thus obtain for stoichiometric YbN an optical mass of $m_0 \cong 2.23m_e$, which is the same order of magnitude as in other strongly covalent rare-earth chalcogenides[22] (GdSe $m_0 = 1.65_e$, GdTe $m_0 = 2.5m_e$). Here we have to admit that the use of N_e taken from a single-band Hall effect can meet with criticism since it is obvious that in a self-compensated semimetal one has at least a two-band model, averaging already over the three valence bands.
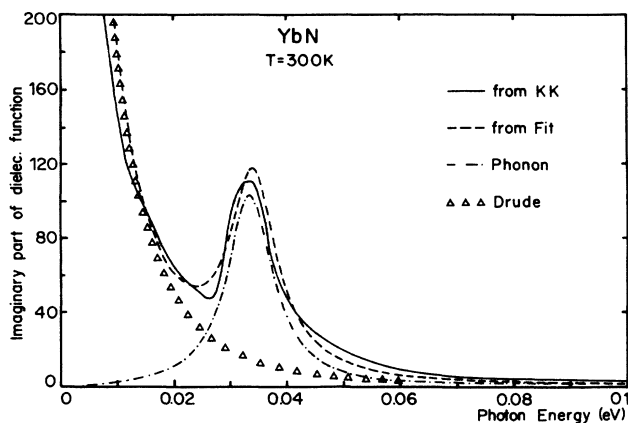

FIG. 6. Imaginary part of the dielectric functions of stoichiometric YbN at 300 K and its decomposition into a Drude and a phonon part.

In a two-band model N_e is normalized by $(\mu_e - \mu_h)/(\mu_e + \mu_h)$, the relative mobilities of electrons and holes, which in turn depend on the band width and the effective mass. But since in Eq. (5) only ratios appear we think that the determination of the effective mass in Eq. (5) is not bad, especially since it is compatible with other rare-earth compounds.[22] Since this mass determination basically comes from an optical measurement and in view of the claim of YbN being a heavy fermion,[12] we especially checked the reflectivity in the far infrared spectral region below the phonon frequencies, also at 6 K, for any anomaly typical of heavy fermions,[23] but everything behaved normally for the stoichiometric sample. Therefore, there is no evidence of a renormalized Drude behavior which would imply an enhanced effective mass.[24] We thus conclude again that perfect YbN is not a heavy fermion and masses of about $50m_e$, which would be needed for a heavy fermion are not conceivable. However, the nonstoichiometric material did indeed show an anomaly in the far infrared spectral region at low temperature which will be discussed subsequently.

Let us turn now to the third term of Eq. (3) which describes the phonons. The decoupling scheme and the fit with a single Lorentzian of the phonon line is shown in Fig. 6. The phonon corresponds to a transverse optical phonon at the Γ point of the Brillouin zone which can be excited by light. The parameters which optimize the phonon part of the spectrum are $\omega_{TO} = 34$ meV , $\Omega = 188$ meV, and $\Gamma = 10$ meV. To obtain the longitudinal optical phonon we realize, of course, that the plasmon and the ω_{LO} phonon couple to become a plasmaron, the resonance of which is where ϵ_1 becomes zero. Of more interest, although not accessible experimentally, is the LO phonon frequency alone which we obtain by decoupling the electron and the phonon contribution and look for the zero crossing of the pure phonon dielectric constant, augmented by ϵ_{opt}. This is at $\omega_{LO} = 62$ meV. Both phonon frequencies are appreciably softened compared with ScN (Ref. 11) ($\omega_{TO} = 45$ meV, $\omega_{LO} = 155$ meV) which is reasonable because of the larger atomic mass of YbN compared with ScN.

Additional information regarding the phonons can be obtained from Fig. 2 where we measured the Raman effect of YbN and compared it with ScN.[11] In these rocksalt-type structures the Raman effect measured a weighted one phonon density of states. In this structure the largest density of states is observed at the L point of the Brillouin zone, i.e., at the zone edge. The optically derived phonon frequencies from the Γ point are thus not directly comparable with Fig. 2, but we obtain additional information. We see again from Fig. 2 that the phonon spectrum of YbN is softened compared with ScN because of the larger mass of Yb relative to Sc. Phonon density-of-states calculations on the comparable compound TiN (Ref. 25) reveal that the peak at 45 meV in YbN corresponds to the acoustic branch with the maximum at the LA and the shoulder at the TA density of states. The optical branch has only one peak at 71 meV corresponding to a LO phonon density of states screened by charge carriers. In principle, the Raman effect can also detect crystal-field excitations of the Γ_6 ground state ($\Gamma_6 \rightarrow \Gamma_8$),

especially observable at low temperatures, when phonon excitations have died out. We failed, however, to detect a reliable signal.

Interband transitions

Now we want to discuss the interband transitions in YbN, i.e., optical transitions above 0.1 eV. Looking at Fig. 1(a) and Fig. 4(a) we observe a peak for stoichiometric YbN at 0.2 eV which has the character of a single Lorentzian line, but is missing in non-stoichiometric YbN. At higher energies and most obvious in Fig. 1(b), Fig. 4(b), and Fig. 5, we find a series of high-energy transitions which shift in energy and intensity when the crystals become nonstoichiometric. By comparison with similar spectra on ScN (Ref. 11) we realize that a transition near 0.2 eV is missing there, whereas otherwise the spectra are nearly identical. To demonstrate this explicitly we plot in Fig. 7 the energy-loss function of $Im(1/\hat{\epsilon})$ of stoichiometric YbN and ScN which exhibits peaks at all resonances, be they phonons, plasmons, or interband transitions. Since the energy loss depends on ϵ_1 and ϵ_2 and displays a peak where both dielectric functions are small, the peaks are not exactly at the same energy as in ϵ_2 or σ_1. The lowest-energy peaks in both compounds are due to phonons, the dominant peaks are the plasmons, and above 0.8 eV the typical p-d interband transitions commence. However, it is obvious that in stoichiometric YbN there is an additional peak compared with ScN at about 0.2 eV. It is reasonable to associate this additional peak with optical transitions involving the $4f$ state. In nonstoichiometric YbN this peak is hardly visible since it is covered by the plasma edge at 0.3 eV because this material has a much higher electron concentration than perfect YbN.

In principle, we now have two possibilities, either a transition from occupied d states below E_F into an empty $4f$ state above E_F, and as such only the $4f^{14}$ state occupied with one hole is conceivable, or a transition from an occupied $4f$ state below E_F, and as such only the multi-electron $4f^{13}$ state is possible, into empty d states above

E_F. (Matrix-element considerations rule out other transitions.)

The occupied bare $4f^{13}$ state in Yb is about 6 eV below E_F (Ref. 10) and we do not expect great changes in YbN. But, in fact, XPS (x-ray photoemission spectroscopy) and BIS (bremsstrahlen isochromate spectroscopy) experiments on the related compound YbP has been performed.[26] The result is shown in Fig. 8 with binding energy negative relative to E_F. XPS spectra from $4f^n$ core levels exhibit the $4f^{n-1}$ multiplets, which are the ^3H_J, ^3F_J, $(^1G,^1D,^1I)$ and ^3P_J of the $4f^{12}$ state giving the fine structure in Fig. 8 below 6 eV binding energy (the singlets involving spin-flip transitions with weaker intensity). The minimum energy for the excitation of a $4f^{13}$ electron into the vacuum (subtracting already the work function) is 6 eV. With this energy no $4f^{12}$ multiplets can be excited and it is thus the position in energy of the $4f^{13}$ level in an energy-level diagram shown in Fig. 9. The small hump between 0 and -4 eV is due to p valence-electron emission and we realize that the p bands extend up to and above the Fermi level. The BIS part of the spectrum of Fig. 8 displays the unoccupied part of the energy levels and for core levels the $4f^{n+1}$ states are shown. For Yb this is the spherically symmetric $4f^{14}$ state, centered at about 1 eV above E_F. For still higher energies we see the d bands which commence right at E_F and overlap slightly with the p valence bands. This figure also demonstrates with its $4f^{14}$ level above and its $4f^{13}$ level below E_F that the compound is not intermediate valent and also not a heavy fermion,[12] because otherwise the Fermi level would be in one of the $4f$ states, as shown, e.g., in the intermediate valent and heavy fermion YbAl$_3$.[27] The exciting and rather unexpected situation is that the unoccupied $4f^{14}$ state (or the one-hole state) is so close to E_F that it can even be thermally populated or that off-stoichiometric samples lead to a certain $4f^{14}$ or Yb^{2+} population. From the experimental point of view we have to realize that the spectral resolution of the BIS spectra is 1 eV and of the XPS spectra 0.3 eV.

Returning back now to the subject of stoichiometric YbN and the optical tranistion at 0.2 eV which involves
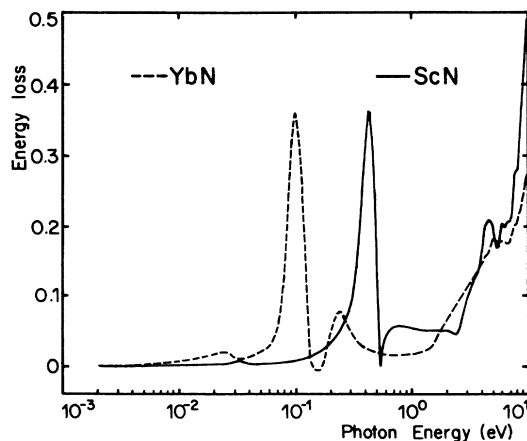

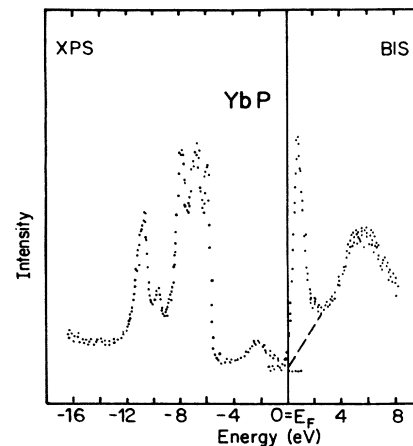FIG. 7. Energy loss spectra of stoichiometric YbN and ScN.
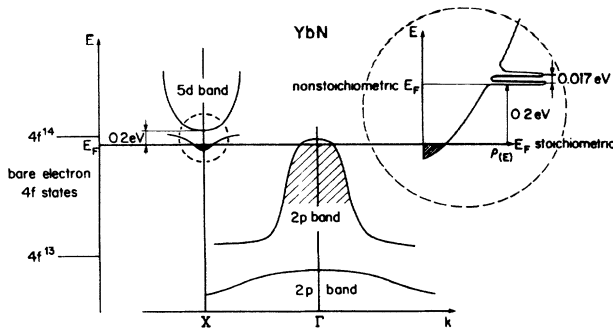

FIG. 8. XPS and BIS spectra of YbP at 300 K (Ref. 26).

FIG. 9. Sketch of an energy-level scheme for YbN. To the left the bare electron $4f$ states are shown. In th middle part of the hybridized band structure is presented, whereas in the right part a magnified sketch of the density of states near E_F is shown.

the f state, we realize now that it can only be the transition from a d electron at E_F into the empty $4f^{14}$ state which we expect to be very close to, but above E_F. This proposal is further supported by the fact that the matrix elements for this transition scale as $1/\omega^2$ which indicates that only low energy (up to about 2 eV) f-d or d-f tranistions can be optically observed with reasonable probability. It is thus only the second time that we can observe and report on optical tranistions into empty $4f$ states; the first time was a transition into an empty $4f^1$ state of tetravalent Ce in CeO_2.[19]

The next higher-energy transitions in both types of YbN are found at 0.4 and 0.8 eV, nearly, but less energy than in ScN^{11}(0.8 eV) and they are direct optical transitions near the X point of the Brillouin zone, consulting the self-consistent band-structure calculation of ScN.[17] In YbN the bare $4f^{13}$ state and the p valence band are mixing (p-f mixing) and due to this hybridization a spectral repulsion with a hybridization gap in the p band occurs,[28] shifting part of the p band closer to the d band. The dominant peak in ϵ_2 or σ_1 is at 2.0 eV (stoichiometric) and 2.2 eV (nonstoichiometric sample) and it corresponds to the direct gap at the Γ point of the Brillouin zone. The shift between the two types of material seems reasonable since the nonstoichiometric material has a nitrogen deficiency and thus less p states, the valence band has a smaller width which increases the tranistion energy. The transitions between 6 and 7 eV correspond to the W point and at 12 eV to the L point. Of course the latter proposals must await a quantitative confirmation from joint density of states and matrix element calculations. However, it is remarkable how the peaks of the interband transitions shift in energy between both compounds and that with only a few percent change in composition. One of the main reasons is that the valence band has a similar width in the nonstoichiometric material but the Fermi level lies higher in the d band. That the optical structure is more pronounced in the non-stoichiometric YbN is the result of *in situ* cleaving compared to polishing (and increased light scattering) in the stoichiometric compound.

In Fig. 9 we finally plot the essence of the electronic structure with band states on the right and localized bare f states on the left where the connection is given by the energy of d-f tranistions and by the Coulomb correlation energy of nearly 6.5 eV between the empty $4f^{14}$ and the occupied multielectron state $4f^{13}$ taken from Fig. 8.

The Kondo effect

We mentioned previously that stoichiometric YbN did not show any anomaly in the far infrared spectral region which we would associate with Kondo, intermediate valent, or heavy fermion characteristics. As such a dip in the reflectivity in the meV range occurring only at very low temperatures would be typical, as in UPt_3 or $CeCu_6$.[23,29] However, it is precisely such a feature which we observe only in nonstoichiometric YbN in the infrared region and at low temperatures and it is depicted in Fig. 1(a), where we observe two peaks at about 17 and 38 meV followed by a deep minimum at about 5 meV, before the reflectivity finally rises towards 100% for $\omega \to 0$. The Kramers-Kronig analysis yields the dielectric constant ϵ_2 which is shown in Fig. 4(a) and we clearly observe two pronounced peaks in the far infrared region, one belonging to the TO phonon, now shifted to 38 meV and the other being at 17 meV. At still lower energies we observe the rise of the dielectric constant due to plasma effects. Again, we have to decouple this plasmon from the phonon and the new oscillator and look for the zero crossing of ϵ_1'. We then obtain the unscreened ω_p as in formula (4), which depends on $(N_e/m_0)^{1/2}$. We now employ the following logic: At room temperature stoichiometric and nonstoichiometric YbN show the same reflectivity features, only ω_p shifts from 0.21 towards 0.5 eV, respectively [Fig. 1(a)]. It is reasonable to assume that at room temperature the optical mass m_0 is for both materials given by the curvature of the bands, and since the concentration of carriers for both materials still is in the percentage range per formula unit the optical mass will be about the same. The shift of the plasma edge between the materials then is only indicative of the change in carrier concentration. We now estimate $N_e \approx 2.7 \times 10^{21}$ cm^{-3} for the nonstoichiometric compound. N_e is practically temperature independent in a semimetal. Thus, at low temperature $\omega_p = 0.3$ eV of the nonstoichiometric compound yields a mass enhancement of about 2.8.[24] Using now the optical mass derived from Eq. (5) at 300 K we can estimate an upper limit of $m_0 \approx 6m_e$ at low temperature for the nonstoichiometric material. Therefore, we observe only a relatively small mass enhancement, which essentially is due to the only small carrier concentration far below that of, e.g., UPt_3 or $CeCu_6$, where it nearly amounts to 1 per formula unit.

As an explanation for these features we have to recall the salient feature of YbN, namely the closeness of the empty $4f^{14}$ (or one-hole state) to the Fermi level and the hybridization of the $4f^{14}$ state with the $5d$ band. For perfect YbN this hybridized $4f^{14}$ state is about 0.2 eV above the Fermi level and it will be empty. We think, however, that this state can be partially occupied in non-stoichiometric YbN which has more free carriers than

ELECTRONIC STRUCTURE OF YbN

the perfect material. Since the total number of free carriers is still in the percent range per formula unit we have a statistical and relatively low population of the $4f^{14}$ state which is precisely the condition for a d-f Kondo effect to occur. The density of states at the Fermi level (which is now at the bottom of the hybridized $4f^{14}$ "band") indicated by the γ value of the specific heat will not be large and thus not typical of a heavy fermion (its experimental determination was not feasible because of the Kondo effect and the magnetic order being manifest in the specific heat (see next paragraph)[12]). The material will be intermediate valent but only to a very poor degree, which, however, can explain the increased lattice constant (4.784 Å) compared with the more perfect material (4.781 Å) because the $4f^{14}$ state has a larger radius than the $4f^{13}$ state.

We now must discuss the significance of the absorption peak at 17 meV which is only present at low temperatures in nonstoichiometric YbN. We have already mentioned the hybridization of the $4f^{14}$ state with the $5d$ band which results in a small hybridization gap. These gaps have been experimentally observed in the far infrared region in intermediate valent SmB_6, the high-pressure phase of SmS, TmSe, and YbB_{12} and in the heavy fermions $UPt_3, CeCu_6$, and U_2PtC_2 (e.g., Refs. 23, 29, and 30). The optical transition across these gaps has reasonable oscillator strengths because of the strong f-d hybridization; the intensity of the absorption structure is so large because it scales with $1/\omega^2$ and the transition is

so far in the infrared region. The density of states calculated from the hybridized f-d states has two pronounced peaks—but only in the nonstoichiometric compound the bottom of the lower peak is populated with some electrons which can perform optical transitions across the gap. This gap then has the experimentally determined size of 17 meV. In the stoichiometric case the optical transition takes place from the Fermi level in the d band to the f density-of-states peaks which is 0.2 eV. In Fig. 9 we try to illuminate the situation in a blown up sketch.

Magnetic properties

Part of the electronic structure is also the ground-state splitting due to the crystalline field and the consequences regarding the magnetic susceptibility, the magnetic order and the specific heat. Since we have established so far that the ground state is $4f^{13}$ and the multiplet $^2F_{7/2}$ we have an eightfold degenerate ground state which splits in the octahedral field into a lower lying Γ_6 doublet, a Γ_8 quartet, and a Γ_7 doublet. The splitting of the ground state can be measured with magnetic susceptibility, neutron scattering, and specific heat—all of which have been done, but only the first two on stoichiometric single crystals.

To confirm the scheme of the crystal-field splitting we analyzed the inverse magnetic susceptibility shown in Fig. 3 with the well-known van Vleck (VV) formula[31] using a cubic crystal field:

$$\chi_{VV} = N\mu_B^2 g^2 \frac{\sum_m \dfrac{\langle \Gamma_m | J_z | \Gamma_m \rangle^2}{k_B T} + 2 \sum_{n \neq m} \dfrac{\langle \Gamma_m | J_z | \Gamma_n \rangle^2}{E_n - E_m} e^{-E_m/k_B T}}{\sum_m p_m e^{-E_m/k_B T}}. \tag{6}$$

Here, N is the number of magnetic ions per mole, μ_B is the Bohr magneton, g is the Landé factor, and E_m the energy of the state Γ_m with the degeneracy p_m. The wave functions for cubic symmetry are taken as

$$\Gamma_6 : a|\pm\tfrac{7}{2}\rangle + b|\mp\tfrac{1}{2}\rangle, \quad \Gamma_7 : c|\pm\tfrac{5}{2}\rangle - d|\mp\tfrac{3}{2}\rangle,$$

$$\Gamma_8 : b|\pm\tfrac{7}{2}\rangle - a|\mp\tfrac{1}{2}\rangle, \quad d|\pm\tfrac{5}{2}\rangle + c|\mp\tfrac{3}{2}\rangle, \tag{7}$$

with $a = (\tfrac{5}{12})^{1/2}$, $b = (\tfrac{7}{12})^{1/2}$, $c = (\tfrac{3}{4})^{1/2}$, and $d = (\tfrac{1}{4})^{1/2}$. Since the measurement yields a paramagnetic Curie temperature different from zero we have to assume an exchange interaction between the magnetic ions. Taking a conventional exchange field $H_E = \lambda M$, with λ a molecular field constant we obtain the measured magnetic susceptibility $1/\chi_m = 1/\chi_{VV} - \lambda$. For high temperatures the inverse magnetic susceptibility follows a Curie-Weiss law with $\mu_{eff} = 4.44 \pm 0.05\mu_B$, only 2% less than the free-ion value of $4.54\mu_B$. The paramagnetic Curie temperature is found as -93.5 K, suggesting antiferromagnetic order. The fit of this theory with the experimental data is shown in Fig. 3 and a very good agreement is obtained with crystal-field parameters $E(\Gamma_6\text{-}\Gamma_8) = 28$ meV and $E(\Gamma_8\text{-}\Gamma_7) = 49.1$ meV. We obtain an overall splitting of 76.7

meV $= 890$ K in comparison with 875 K for nonstoichiometric YbN[4], which seems an excellent agreement; however, in Ref. 4 the $\Gamma_6\text{-}\Gamma_8$ splitting has been calculated to be 48 meV. So far we do not have any difficulties in interpreting YbN in a conventional single-ion crystal-field scheme and also for the magnetic properties there is no reason to assume a heavy-fermion character.[12] However, there is a slight minimum in the reciprocal magnetic susceptibility near 6 K. In fact this phenomenon can already be observed in Ref. 4. This prompted us to measure also the initial susceptibility in a field of 10 Oe, which confirmed these findings inasmuch as the susceptibility flattened out below 6 K, as anticipated for magnetic order. However, a first neutron scattering experiment down to 1.5 K did not show any sign of magnetic order.[32]

However, looking at Ref. 12 where the specific heat of the Yb monopnictides has been measured, we conspicuously observe very pronounced peaks below 1 K, for YbN at 0.735 K. Since it is suggestive to correlate these peaks with magnetic-order elastic and inelastic neutron scattering has been performed on the very same stoichiometric single crystal which we used in our experiment.[32] Indeed, antiferromagnetic order Af III has been observed

with a Néel temperature practically coinciding with the peak temperature of the specific heat. Thus, T_n of YbN would be the same order of magnitude as in another $4f^{13}$ system, namely divalent TmTe, which is a low gap semiconductor.[32] In addition crystal-field excitations $E(\Gamma_6\text{-}\Gamma_8)=30$ meV and $E(\Gamma_8\text{-}\Gamma_7)=45$ meV have been found in excellent agreement with our determination from the magnetic susceptibility.

Specific heat

The specific heat of YbN has been measured on relatively nonstoichiometric polycrystalline samples[5] (actually the same samples as in Ref. 4) having a lattice constant of 4.792 Å. A Schottky type anomaly was found near 180 K and when this anomaly is associated with the $\Gamma_6\text{-}\Gamma_8$ transition we compute a splitting of 40 meV in relatively poor agreement with the splitting obtained from the analysis of the magnetic susceptibility or inelastic neutron scattering[32] on more perfect material. In the same paper[5] written in 1969 another anomaly in the specific heat of YbN has been found at 3.8 K—the origin of which was not clear. In a more recent paper the same anomaly has been observed at about 5 K,[12] again on nonstoichiometric samples with a lattice constant of 4.784 Å, in addition to the λ-type anomalies of 0.735 K due to the antiferromagnetic order. The anomaly at about 5 K prompted the authors[12] to propose a heavy-fermion characteristic of YbN.

In a very recent paper[28] the specific heat of the Yb pnictides has been analyzed theoretically using the $p\text{-}f$ mixing already postulated for the crystal-field split states as well. As a result the authors demonstrate that the $p\text{-}f$ Kondo effect is responsible for a maximum in the specific heat in the Yb pnictides—for YbN at about 5 K—the estimated Kondo temperature. We now realize also that the unusual behavior of the initial susceptibility, reported above, with a weak maximum near 6 K has the same origin in the $p\text{-}f$ mixing—only this measurement was performed on a stoichiometric sample.

CONCLUSION

For the first time we have been able to grow stoichiometric single crystals of YbN and prove it by chemical analysis. These crystals have, with 4.781 Å, the smallest lattice constant ever measured which we associate with a nearly (weakly hybridized) pure $4f^{13}$ ground state without any population of a (larger) $4f^{14}$ state. On these crystals a series of physical measurements like optical spectroscopy, Raman effect, electrical conductivity, Hall effect, magnetization, and neutron scattering has

been performed. The main results are that the material is a self-compensated semimetal with the p band at Γ and the d band at X having an indirect overlap, producing equal numbers of electrons and holes with a concentration of percents per formula unit. The effective optical mass of the carriers could be determined to be about $m_0 \approx 2.2 m_e$ which is quite normal for these covalent compounds. The bare $4f^{13}$ state is found by photoemission to be about 6 eV below E_F and its overlap with the p band results in a $p\text{-}f$ mixing or hybridization. This in turn results in a $p\text{-}f$ Kondo effect in the $^2F_{7/2}$ Γ_6 ground state which can explain the anomalies in the magnetic susceptibility near 6 K and in the specific heat near 5 K.

The salient and unexpected feature of YbN, however, is the position of the empty $4f^{14}$ (or one hole) state about 0.2 eV above the Fermi level as evidenced by BIS and optical spectroscopy. This $4f^{14}$ state hybridizes with the empty $5d$ band and results in a narrow hybridization gap. Since these levels are unoccupied in the stoichiometric compound we do not expect much influence on physical properties. However, when the material becomes nonstoichiometric we measure a larger carrier concentration so that the Fermi level enters the hybridized $4f^{14}$ state somewhat resulting in a $f\text{-}d$ Kondo effect in addition to the $p\text{-}f$ Kondo effect already being present. This leads to a mass enhancement of the effective optical mass of about 2.8–3, to an increased lattice constant, and to an additional optical transition in the far infrared across this hybridization gap of 17 meV. Also, stoichiometric YdN as nonstoichiometric YbN are not heavy fermions. However, with applied hydrostatic pressure or alloying with tetravalent metals the carrier concentration in the $4f^{14}$ state can probably be enhanced so much that this state becomes significantly occupied–perhaps as much as the density-of-states maximum, resulting in a large effective mass, an enhanced γ value of the specific heat, and finally heavy-fermion characteristics. These experiments are left for the future.

[1] L. Davis, Conference on Rare Earths and Actinides, Durham, 1971 [N.C. Digest 2, 126 (1971)].

[2] A. Narita and T. Kasuya, J. Magn. Magn. Mater. 52, 373 (1985).

[3] H. Harima and T. Kasuya, J. Magn. Magn. Mater. 52, 370 (1985).

[4] P. Junod, A. Menth, and O. Vogt, Phys. Kondens. Materie 8, 323 (1969).

[5] W. Stutius, Phys. Kondens. Materie 10, 152 (1969).

[6] N. Sclar, J. Appl. Phys. 35, 1534 (1964).

[7] P. Wachter and E. Kaldis, Solid State Commun. 34, 241 (1980).

[8] A. Schlegel, PhD Thesis, Eidgenössische Technische

Hochschule, Zürich, 1979.

[9]P. Wachter, E. Kaldis, and R. Hauger, Phys. Rev. Lett. **21**, 1404 (1978).

[10]P. A. Cox, Y. Baer, and C. K. Jorgensen, Chem. Phys. Lett. **22**, 433 (1973).

[11]G. Travaglini, F. Marabelli, R. Monnier, E. Kaldis, and P. Wachter, Phys. Rev. B **34**, 3876 (1986).

[12]H. R. Ott, H. Rudigier, and F. Hulliger, Solid State Commun. **55**, 113 (1985).

[13]T. Greber, L. Degiorgi, R. Monnier, L. Schlapbach, F. Hulliger, and E. Kaldis, J. Phys. (Paris) Colloq. **48**, C9-943 (1987).

[14]E. Kaldis, B. Steinmann, B. Fritzler, E. Jilek and A. Wisard, in *The Rare Earths in Modern Science and Technology*, edited by J. McCarthy *et al.* (Plenum, New York, 1982), Vol. 3, p. 224.

[15]E. Kaldis and Ch. Zürcher, in *Proceedings of the Twelfth Rare Earth Research Conference, Denver, 1976*, edited by C. E. Lundin (Denver Research Institute, Denver, 1976), p. 915.

[16]A. Neckel, P. Rastl, R. Eibler, P. Weinberger, and K. Schwarz, J. Phys. C **9**, 579 (1976).

[17]R. Monnier, J. Rhyner, T. M. Rice, and D. D. Koelling, Phys. Rev. B **31**, 5554 (1985).

[18]A. Furrer and W. Hälg, J. Phys. C **9**, 3499 (1976).

[19]F. Marabelli and P. Wachter, Phys. Rev. B **36**, 1238 (1987).

[20]D. D. Koelling, A. M. Boering, and J. H. Wood, Solid State Commun. **47**, 227 (1983).

[21]R. Hauger, E. Kaldis, G. von Schulthess, P. Wachter, and Ch. Zürcher, J. Magn. Magn. Mater. **3**, 103 (1976).

[22]W. Beckenbaugh, J. Evers, G. Güntherodt, E. Kaldis, and P. Wachter, J. Phys. Chem. Solids **36**, 239 (1974).

[23]F. Marabelli, G. Travaglini, P. Wachter, and J. J. M. Franse, Solid State Commun. **59**, 381 (1986).

[24]A. M. Awasthi, W. P. Beyermann, J. P. Carini, and G. Grüner, Phys. Rev. B **39**, 2377 (1989).

[25]W. Kress, P. Roedhammer, H. Bilz, W. D. Teuchert, and A. N. Christensen, Phys. Rev. B **17**, 111 (1978).

[26]E. Wuilloud, PhD. thesis, University de Neuchatel, Neuchatel, 1986.

[27]M. Campagna, G. K. Wertheim, and Y. Baer, in *Photoemission in Solids II*, Vol. 27 of *Topics in Applied Physics*, edited by L. Ley and M. Cardona (Springer-Verlag, Berlin, 1979), p. 217.

[28]R. Monnier, L. Degiorgi, and B. Delley, Phys. Rev. B **41**, 573 (1989).

[29]F. Marabelli, P. Wachter, and E. Walker, Phys. Rev. B **39**, 1407 (1989).

[30]G. Travaglini and P. Wachter, Phys. Rev. B **29**, 893 (1984).

[31]M. M. Schieber, in *Experimental Magnetochemistry*, Vol. VIII of *Selected Topics in Solid State Physics*, edited by E. P. Wohlfarth (North-Holland, New York, 1967).

[32]A. Furrer, P. Fisher, and A. Dönni (private communication).

[33]P. Wachter, Lanthanide and Actinide Research **1**, 265 (1986).